

Bayesian Flow Is All You Need to Sample Out-of-Distribution Chemical Spaces

Nianze TAO*

*Department of Chemistry, Graduate School of Advanced Science and Engineering,
Hiroshima University, 1-3-1 Kagamiyama, Higashi-Hiroshima, Japan 739-8524*

E-mail: tao-nianze@hiroshima-u.ac.jp

Abstract

Generating novel molecules with higher properties than the training space, namely the out-of-distribution generation, is important for *de novo* drug design. However, it is not easy for distribution learning-based models, for example diffusion models, to solve this challenge as these methods are designed to fit the distribution of training data as close as possible. In this paper, we show that Bayesian flow network is capable of effortlessly generating high quality out-of-distribution samples that meet several scenarios. We introduce a semi-autoregressive training/sampling method that helps to enhance the model performance and surpass the state-of-the-art models.

Introduction

The chemical space is large, and even the sub-space is too large to be explored completely. For instance, the number of *small* drug-like molecules is believed to be over 10^{60} ,¹⁻³ amongst which, however, only a much smaller sub-region, e.g., macrocycles,⁴⁻⁶ were tested in the laboratories and applied into real world challenges; when we start considering larger systems like proteins, the space grows exponentially.⁷

Recent emerging deep generative models that virtually search the chemical space are attractive alternatives to trial-and-error processes conducted by human scientists.^{8–12} Despite the success of generative models, especially the distributional learning models, in molecule generation, some researchers have pointed out the limitations of these methods: because the models and benchmarks were designed to optimise and test the in-distribution performance, i.e., how *close* the generated molecules are to the training data, (1) the models were pool at generating highly novel samples with desired properties;^{9,13} (2) multi-objective optimisation was difficult;⁹ (3) the sampling space could change to the false-positive region volatiley when an overconfident guidance appeared.¹⁴ To overcome these problems, it is important to improve the performance of out-of-distribution (OOD) generation, i.e., generating compounds with higher properties than that of molecules in the training dataset.

Pioneering works have introduced a few methods to enhance the diffusion models' OOD performance including introducing a dedicatedly designed control method to steer towards the OOD space,⁹ and utilising unlabelled data to increase the training domain and regularise the model.¹⁴ In this research, we, on the other hand, show that the Bayesian flow network, another branch of deep generative methods, is a *natural* out-of-distribution sampler. Moreover, we demonstrate that by introducing a semi-autoregressive behaviour our method outperformed several state-of-the-art (SOTA) models in OOD multi-objective optimisation tasks.

Methods

Bayesian Flow Networks

Similar to denoising diffusion models^{15–20} (DMs) and more general flow matching methods,^{21–29} Bayesian flow networks³⁰ (BFNs) splits the generative process to a sequential steps. Some research has pointed out that the generative process of BFN is similar to thus can be approximated as a reversed stochastic differential equation (SDE) that used in DMs though,^{31,32}

BFN method does not require to define a diffusion process nor learns the noise distribution: instead, BFN directly optimises the parameters of a distribution towards a more informative direction, which makes it applicable to continuous, discretised, and discrete data as the *parameters* of any real-world distribution is continuous.³⁰ The previous studies have already applied the idea of BFN to 3-dimensional molecular conformation generation^{33,34} (discretised and continuous case), text-based molecule generation³⁵ (discrete case), and protein sequence generation³² (discrete case), which proved its capability of understanding the chemical space. In this research, we employ ChemBFN,³⁵ a BFN model handling the 1-dimensional molecular representation originally designed to generate SMILES³⁶ and SELFIES³⁷ strings, to study BFN’s potentials of out-of-distribution sampling, i.e., generating samples with high properties out of a low-property training space. We show that a small change in the training or sampling process of ChemBFN can significantly enhance the out-of-distribution generative performance.

Efficient Sampling with BFN

Although ChemBFN succeeded in generating diverse molecules, the ratio of valid SMILES was low when fewer sampling steps was used.³⁵ To reduce the sampling steps while retaining the high validity ratio, here we propose two methods.

I. Auxiliary reinforcement learning term. We define the following reinforcement learning (RL) term, inspired by REINFORCE algorithm,^{38,39} added into the training loss

$$L^{RL} = \eta \mathbb{E}_{t \sim U(0,1)} \left(\mathbf{e}^{(k)}(\hat{\boldsymbol{\theta}}; t) \cdot (1 - \delta_c(\mathbf{e}(\hat{\boldsymbol{\theta}}; t))) \right), \quad (1)$$

where η is a scaling constant, $k = \text{argmax}(\mathbf{e}(\hat{\boldsymbol{\theta}}; t))_{\text{dim}=-1}$, $\mathbf{e}(\hat{\boldsymbol{\theta}}; t)$ is the estimated categorial distribution (i.e., output distribution in terms of BFN) at time t via the neural network, and $\delta_c(.) = 1$ when criterion c is satisfied but 0 elsewhere. To increase valid ratio of generated molecules, a naïve strategy is to raise the possibilities that at any time step t the

output distributions correspond to valid molecules. Therefore, we set the criterion c as $c := \{\mathbf{e}(\hat{\boldsymbol{\theta}}; t) \text{ corresponds to a valid molecule}\}$. In practice, we found that $\eta = 0.01$ was optimal in most cases while $\eta < 0.001$ or $\eta > 0.1$ led to degraded performance.

II. ODE-like generating process. The linkage between SDE and BFN generating process was first discovered by K. Xue *et al.*³¹ who stated that by directly operating in the latent space Ω_z instead of the distribution parameter space Ω_θ , an ordinary differential equation (ODE) solver or a SDE solver that updated the latent variable $\mathbf{z}_i = \mathbf{z}_{i-1} + \alpha_i(K\mathbf{e}(\hat{\boldsymbol{\theta}}_{i-1}; t_{i-1}) - 1) + \sqrt{K\alpha_i}\boldsymbol{\epsilon}$ (where $\mathbf{z} \in \Omega_z$, $\boldsymbol{\theta} \in \Omega_\theta$, $\boldsymbol{\epsilon} \sim \mathcal{N}(\mathbf{0}, \mathbf{I})$, and K is the number of categories) could accelerate the generating process. A simplified alternative method proposed by T. Atkinson *et al.*³² reduced the complexity of the algorithm, based on which we found that scaling the randomness by a temperature coefficient $\tau > 0$ further benefited the valid ratio of generated objects. Our ODE-like sampling algorithm is shown in Algorithm 1.

In the later text, we show that the combination of these two method significantly speeds up the molecular generation.

Algorithm 1 ODE-like sampling algorithm

Require: $\tau > 0$, conditioning $\mathbf{y} \in \mathbb{R}^f \cup \phi$, $n, K \in \mathbb{N}$, accuracy schedule $\beta(t)$

```

 $\mathbf{z} \leftarrow \mathbf{0}$ 
for  $i = 1$  to  $n$  do
   $t \leftarrow (i - 1)/n$ 
   $s \leftarrow t + 1/n$ 
   $\boldsymbol{\theta} \leftarrow softmax(\mathbf{z})_{dim=-1}$ 
   $\boldsymbol{\epsilon} \sim \mathcal{N}(\mathbf{0}, \mathbf{I})$ 
   $\mathbf{e}(\hat{\boldsymbol{\theta}}; t) \leftarrow \text{DISCRETE\_OUTPUT\_DISTRIBUTION}(\boldsymbol{\theta}, t, \mathbf{y})$ 
   $\mathbf{z} \leftarrow \beta(s)(K\mathbf{e}(\hat{\boldsymbol{\theta}}; t) - 1) + \sqrt{K\beta(s)}\tau\boldsymbol{\epsilon}$ 
end for
 $\boldsymbol{\theta} \leftarrow softmax(\mathbf{z})_{dim=-1}$ 
 $\mathbf{e}(\hat{\boldsymbol{\theta}}; 1) \leftarrow \text{DISCRETE\_OUTPUT\_DISTRIBUTION}(\boldsymbol{\theta}, 1, \mathbf{y})$ 
return  $\text{argmax}(\mathbf{e}(\hat{\boldsymbol{\theta}}; 1))_{dim=-1}$ 

```

Semi-autoregressive Training and Sampling

In the original ChemBFN³⁵ model and any BERT⁴⁰-like model, tokens are updated bidirectionally as illustrated in Figure 1 (left), where for an arbitrary token in a finite fixed-length sequence $s_j \in (s_0, s_1, s_2, \dots, s_N)$ a function f_{BI} maps s_j from i^{th} layer to $(i + 1)^{th}$ layer based on itself and tokens from both left side (previous tokens) and right side (subsequent tokens), i.e., $s_j^{i+1} = f_{BI}(s_j^i; s_{0:j-1}^i, s_{j+1:N}^i)$. In the case of autoregressive models, however, since the sequence is extended step by step (as shown in Figure 1 (middle)), the next token s_{j+1} only comes from the previous tokens via a function f_{AR} , i.e., $s_{j+1}^{i+1} = f_{AR}(s_{0:j}^i)$. For models employing self-attention mechanism, e.g., the decoder of autoencoder transformer⁴¹ model and GPT⁴² model, a causal mask that maps entities of the attention matrix above the main diagonal to zero is applied to implement this autoregressive behaviour. We found that in a trained ChemBFN model, the entities that were far away from the main diagonal in the attention matrices were extremely close to zero, which enlightened the possibility of applying causal masks to ChemBFN models without breaking models' generative capability. By employing the causal mask, we introduce a semi-autoregressive (SAR) behaviour to ChemBFN models, in which all tokens are updated together as a block but subsequent tokens are not used to update the current token (Figure 1 (right)), i.e., $s_j^{i+1} = f_{SAR}(s_j^i; s_{0:j-1}^i)$.

To be simple, we denote applying causal masks to models as 'SAR' while 'normal' stands for disenabling causal masks. Depending on whether the causal masks are used in training or sampling processes, four strategies (strategy 1 - 4) are proposed in Table 1. We show how these settings affect the generative behaviours of our model in later texts.

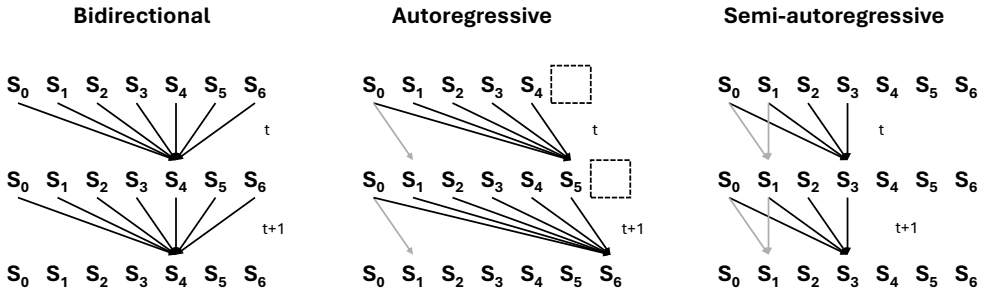


Figure 1: Visualisation of bidirectional, autoregressive, and semi-autoregressive token update methods.

Table 1: Training and sampling strategies^a

Strategy	Training	Sampling
1	normal	normal
2	normal	SAR
3	SAR	normal
4	SAR	SAR

^a SAR is ‘semi-autoregressive’.

Datasets and Benchmarks

MOSES⁴³ as well as GuacaMol⁴⁴ are widely-used benchmarks in the studies of small molecule generation. Apart from testing the validity, uniqueness, diversity, and novelty of generated molecules, MOSES benchmark focuses more on the distribution learning performances of tested models, including Tanimoto similarity (SNN), fragment similarity (Frag), scaffold similarity (Scaf), and Fréchet ChemNet Distance⁴⁵ (FCD). Although the purpose of MOSES is to estimate how *close* the learnt distribution is to the training space, in the study it was utilised to showcase how *far away* the generated space of our method could be from the training space while retaining the chemical meaningfulness.

Lee *et al.*⁹ on the other hand, proposed ZINC250k dataset, which is consisted of 249,455 molecules collected from ZINC⁴⁶ database and their paired quantitative estimate of drug-

likeness⁴⁷ (QED), synthetic accessibility⁴⁸ (SA), and docking scores (DS) unit in kcal/mol to five different proteins (PARP1, FA7, 5HT1B, BRAF, and JAK2) calculated via QuickVina 2,⁴⁹ and the corresponding metrics to test the OOD multi-objective guided molecular generating performance. In this benchmark, a group of filters that should be applied to generated molecules are defined as

$$\left\{ \begin{array}{l} \text{QED} > 0.5 \\ \text{SA} < 5 \\ \text{DS} < \widetilde{DS}(\text{molecules in training data}) \\ \text{SNN} < 0.4, \end{array} \right. \quad (2)$$

where \widetilde{DS} stands for median value of docking score and SNN is the Margon fingerprint Tanimoto similarity to the nearest neighbour in the training set. The two metrics, *novel hit ratio* and *novel top 5% docking score*, are therefore defined as

$$\left\{ \begin{array}{l} \text{Novel hit ratio} = \frac{\text{Nº molecules passed all the filters}}{\text{Nº generated molecules}} \times 100\% \\ \text{Novel top 5% docking score} = \overline{DS}(\text{top 5% molecules passed all the filters}). \end{array} \right. \quad (3)$$

According to Lee *et al.*,⁹ it is recommended to sample 3,000 molecules for each target protein and to repeat the experiment for 5 times to obtain the mean and standard deviation of the metrics.

Apart from studying the small molecule generating, we further employed a labelled protein dataset (90,990 sequences in the training set) published by N. Gruver *et al.*⁵⁰ to test our method on the generative tasks of larger systems. Amongst several structure-related labels, we selected the percentage of beta sheets and solvent accessible surface area (SASA) as the objective targets as suggested by N. Gruver *et al.*⁵⁰

Experiments and Results

In this section we demonstrated how different training and sampling strategies (defined in the section of Semi-autoregressive Training and Sampling) affected generated spaces of unconditional cases, and then quantified the performance of our model in OOD multi-object optimisations. The improvement of sampling quality from our online reinforcement learning method and ODE-like generating process was presented as well.

Fast Sampling

Table 2: Metrics of MOSES and GuacaMol benchmarks when different numbers of sampling steps and methods were employed^a

Methods	Step	MOSES				
		Valid \uparrow	Unique@1k \uparrow	Unique@10k \uparrow	Filter \uparrow	Novelty \uparrow
ChemBFN ³⁵	1k	0.916 \pm 0.001	1.0 \pm 0.0	0.998 \pm 0.000	0.987 \pm 0.001	0.880 \pm 0.002
ChemBFN ³⁵	100	0.911 \pm 0.002	1.0 \pm 0.0	0.998 \pm 0.000	0.985 \pm 0.001	0.884 \pm 0.002
ChemBFN + RL	100	0.928 \pm 0.002	1.0 \pm 0.0	0.999 \pm 0.000	0.987 \pm 0.000	0.922 \pm 0.001
ChemBFN ³⁵	10	0.835 \pm 0.003	1.0 \pm 0.0	0.999 \pm 0.000	0.976 \pm 0.001	0.921 \pm 0.002
ChemBFN + RL	10	0.852 \pm 0.001	1.0 \pm 0.0	0.999 \pm 0.000	0.977 \pm 0.000	0.946 \pm 0.002
ChemBFN + ODE	10	0.946 \pm 0.000	1.0 \pm 0.0	0.996 \pm 0.001	0.990 \pm 0.000	0.838 \pm 0.003
ChemBFN + RL + ODE	10	0.949 \pm 0.001	1.0 \pm 0.0	0.998 \pm 0.000	0.992 \pm 0.000	0.873 \pm 0.002

		GuacaMol		
		Valid \uparrow	Unique \uparrow	Novelty \uparrow
ChemBFN ³⁵	1k	0.807 \pm 0.003	0.818 \pm 0.001	0.975 \pm 0.001
ChemBFN + RL	10	0.826 \pm 0.003	0.821 \pm 0.003	0.982 \pm 0.000
ChemBFN + ODE	10	0.879 \pm 0.003	0.806 \pm 0.005	0.939 \pm 0.002
ChemBFN + RL + ODE	10	0.863 \pm 0.003	0.820 \pm 0.002	0.980 \pm 0.000

^a The training and sampling followed strategy 1. \uparrow stands for the higher the better. $\tau = 0.5$ for MOSES and $\tau = 0.05$ for GuacaMol when ODE-like generative method was applied.

To compare with the baseline, i.e., the native ChemBFN model, we trained two ChemBFN models from scratch combined with the online RL described in Methods on MOSES and GuacaMol datasets respectively, then sampled the SMILES molecular representation with native BFN method and ODE-like approach. The main results were summarised in Table 2. We observed that (1) RL strategy marginally improved the validity and diversity (uniqueness and novelty) of generated samples; (2) ODE-like sampling strategy helped to drastically increase the validity in the cost of diversity; (3) the combination of RL and ODE-like generating process was the optimal strategy to outperform the baseline in validity while retaining

the high diversity even when the number of sampling steps was reduced from 1k to 10. We also found that (not shown in Table 2) the temperature τ strongly controlled the trade-off between sample quality (validity) and diversity: a $\tau < 0.01$ could lead to validity $\geq 99.5\%$ but the ratio of unique molecules $< 60\%$; when $\tau = 1$ the novelty was high but the validity was in the same level of native BFN sampling. In practice, $\tau = 0.5$ is a value that balances validity and diversity when the sizes of molecules in the training data are highly homogeneous, otherwise the temperature needs reducing to as low as 0.02. Overall, ChemBFN + RL + ODE-like sampling strategy is capable of generating one valid SMILES string within 10.5 to 11.6 steps, which makes it possible to run on a laptop without GPUs. However, we admit the limitation of auxiliary RL that requires 30% more training time at most.

Unconditional Generation of Small Molecules

The MOSES testing metrics of ChemBFN using different strategies were visualised in Figure 2 and the 2-dimensional UMAP⁵¹ plots of unconditional sample spaces of models trained on ZINC250k dataset against the training space were shown in Figure 3. It is clear that diversity and structure related metrics did not significantly response to the change of training and/or sampling strategies, which indicated that SAR process did not worsen the model’s capability of learning molecular structures. The key observation was that the OOD-ness indicated by the magnitude of FCD was strongly affected by different strategies. Figure 3 and Figure 5 (a) further showed that the sample spaces were *far away* from the training space while changing training and/or sampling strategies led the model to explore different OOD spaces.

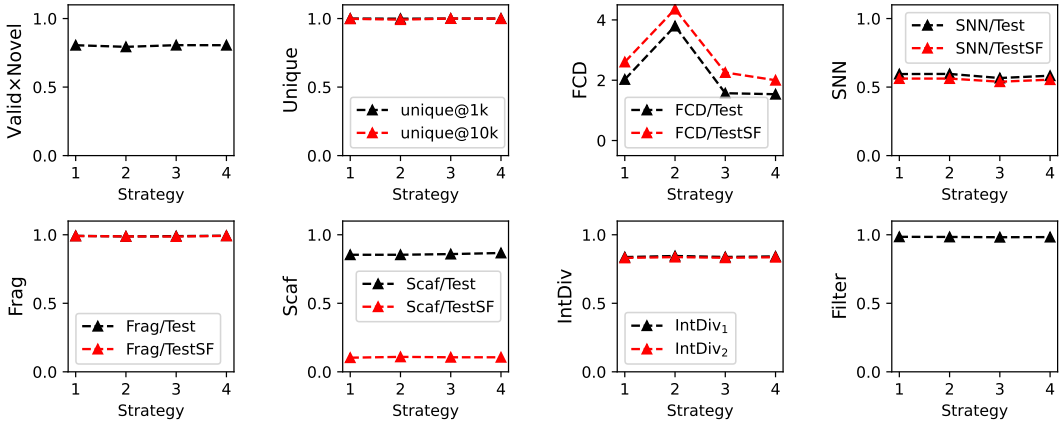


Figure 2: Visualisation of MOSES benchmark metrics of different strategies. We reported Valid \times Novel values instead of validity and novelty separately.

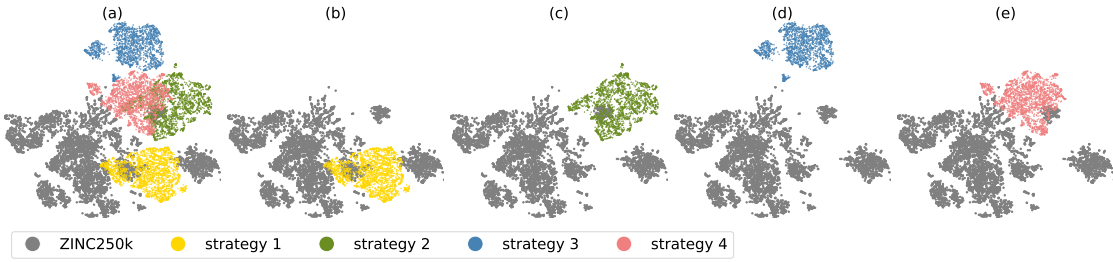


Figure 3: UMAP visualisation of the training space of ZINC250k dataset and the unconditionally generated sample spaces of different strategies.

Conditional Generation of Small Molecules

When a guidance vector $\mathbf{y} = (\text{QED}, \text{SA}, \text{DS})$ pointing to a higher-property space than training space, i.e., high drug-likeness, low synthetic difficulty and more negative docking affinity, was applied to the sampling process via the classifier-free guidance method,⁵² we observed that the sample spaces had a tendency to be close to each other regardless the change of strategy (Figure 4). The OOD-ness was significantly larger than unconditional cases (Figure 5).

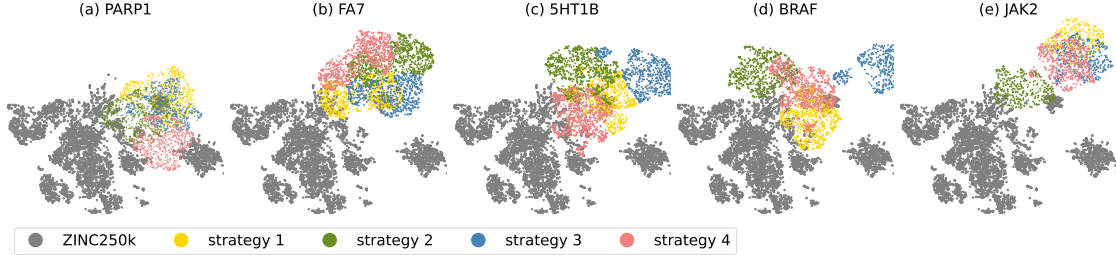


Figure 4: UMAP visualisation of the training space of ZINC250k dataset and the conditionally generated sample spaces of different strategies.

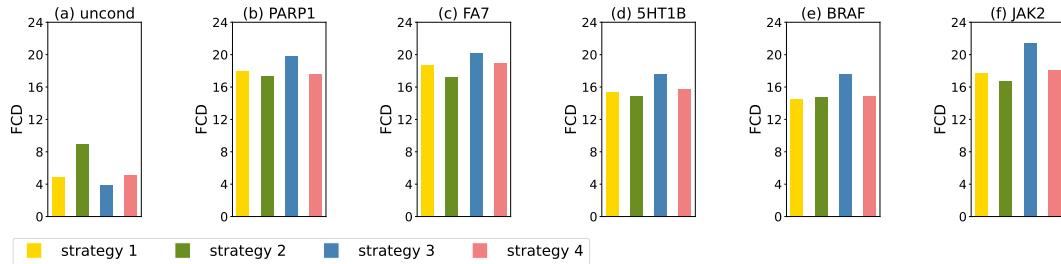


Figure 5: FCD values of unconditional and conditional samples of different strategies.

In Table 3 and Table 4, we summarised the novel hit ratios and novel top 5% docking scores of ChemBFN when different training and/or sampling strategies were applied compared with the SOAT models^{9,53–57} (note that the data of the SOTA models were provided by Lee et al⁹). Regarding to the novel hit ratio, ChemBFN coupled with strategy 4 gave the best results on 4 out of 5 tasks amongst ChemBFN family, which, however, only outperformed the best method on 2 out of 5 tasks. Conversely, all our models outperformed all the SOTA methods for all 5 tasks when concerning the novel top 5% docking scores, amongst which ChemBFN coupled with strategy 3 showed the best performance and strategy 4 presented the second best results.

Table 3: Novel hit ratios (\uparrow) compared with SOTA models^a

Methods	PARP1	FA7	Target proteins		JAK2
			5HT1B	BRAF	
REINVENT ⁵³	0.480 \pm 0.344	0.213 \pm 0.081	2.453 \pm 0.561	0.127 \pm 0.088	0.613 \pm 0.167
MORLD ⁵⁴	0.047 \pm 0.050	0.007 \pm 0.013	0.880 \pm 0.735	0.047 \pm 0.040	0.227 \pm 0.118
HierVAE ⁵⁵	0.553 \pm 0.214	0.007 \pm 0.013	0.507 \pm 0.278	0.207 \pm 0.220	0.227 \pm 0.127
FREED ⁵⁶	3.627 \pm 0.961	1.107 \pm 0.209	<u>10.187</u> \pm 3.306	2.067 \pm 0.626	4.520 \pm 0.673
GDSS ⁵⁷	1.933 \pm 0.208	0.368 \pm 0.103	4.667 \pm 0.306	0.167 \pm 0.134	1.167 \pm 0.281
MOOD ⁹	7.017 \pm 0.428	0.733 \pm 0.141	18.673 \pm 0.423	5.240 \pm 0.285	9.200 \pm 0.524
ChemBFN strategy 1	5.040 \pm 0.473	<u>5.827</u> \pm 0.475	3.100 \pm 0.264	5.340 \pm 0.341	3.973 \pm 0.253
ChemBFN strategy 2	4.660 \pm 0.302	5.567 \pm 0.153	3.653 \pm 0.248	<u>5.293</u> \pm 0.529	4.040 \pm 0.240
ChemBFN strategy 3	4.287 \pm 0.303	4.520 \pm 0.383	3.860 \pm 0.089	3.160 \pm 0.314	4.093 \pm 0.368
ChemBFN strategy 4	<u>5.593</u> \pm 0.417	5.853 \pm 0.423	4.587 \pm 0.358	4.233 \pm 0.518	<u>5.260</u> \pm 0.314

^a The best results are in **bold** and the second best results are underlined. \uparrow stands for the higher the better. We sampled the molecules for 1,000 steps in **SMILES** format. The results were the average values of 5 runs with the standard deviation reported.

Table 4: Novel top 5% docking scores (\downarrow) compared with SOTA models^a

Methods	PARP1	FA7	Target proteins		JAK2
			5HT1B	BRAF	
REINVENT ⁵³	-8.702 \pm 0.523	-7.205 \pm 0.264	-8.770 \pm 0.316	-8.392 \pm 0.400	-8.165 \pm 0.277
MORLD ⁵⁴	-7.532 \pm 0.260	<u>-6.263</u> \pm 0.165	<u>-7.869</u> \pm 0.650	-8.040 \pm 0.337	-7.816 \pm 0.133
HierVAE ⁵⁵	-9.487 \pm 0.278	-6.812 \pm 0.274	-8.081 \pm 0.252	-8.978 \pm 0.525	-8.285 \pm 0.370
FREED ⁵⁶	-10.427 \pm 0.177	-8.297 \pm 0.094	-10.425 \pm 0.331	-10.325 \pm 0.164	-9.624 \pm 0.102
GDSS ⁵⁷	-9.967 \pm 0.028	<u>-7.775</u> \pm 0.039	-9.459 \pm 0.101	-9.224 \pm 0.068	-8.926 \pm 0.089
MOOD ⁹	-10.865 \pm 0.113	-8.160 \pm 0.071	-11.145 \pm 0.042	-11.063 \pm 0.034	-10.147 \pm 0.060
ChemBFN strategy 1	<u>-12.932</u> \pm 0.159	-9.186 \pm 0.149	-12.493 \pm 0.313	-11.955 \pm 0.143	-11.792 \pm 0.337
ChemBFN strategy 2	-12.528 \pm 0.205	-8.925 \pm 0.083	-11.912 \pm 0.265	-11.728 \pm 0.103	-11.677 \pm 0.169
ChemBFN strategy 3	-13.040 \pm 0.211	-9.611 \pm 0.154	<u>-12.448</u> \pm 0.241	-12.350 \pm 0.641	-12.111 \pm 0.275
ChemBFN strategy 4	-12.741 \pm 0.205	<u>-9.442</u> \pm 0.074	-12.275 \pm 0.120	-11.969 \pm 0.203	<u>-12.022</u> \pm 0.120

^a \downarrow stands for the lower the better while other settings are the same as Table 3

We found that when a guidance vector pointing to a higher-property space than training space is applied, the ratio of invalid SMILES³⁶ strings generated by the models increased drastically. To reduce the influence of hallucinations, we additional trained two models: ChemBFN + RL + ODE and ChemBFN + SELFIES.³⁷ The results were shown in Table 5, Table 6, Table 7 and Table 8. The novel hit ratio for all target proteins, as shown in Table 5 and Table 7, increased in both cases: ChemBFN + RL + ODE surpassed SOTA models in 4 out of 5 tasks even when the number of sampling steps was reduced from 1k to 100; for ChemBFN + SELFIES, the ratio significantly improved from less than 6% to over 25%, which outperformed all the SOTA models. The novel top 5% docking scores dropped slightly

as shown in Table 6 and Table 8. Nevertheless, our models still surpassed SOTA methods.

Table 5: Novel hit ratios (\uparrow) of ChemBFN + RL + ODE-like sampling ($\tau = 0.5$) compared with SOTA models^a

Methods	PARP1	FA7	Target proteins		
			5HT1B	BRAF	JAK2
REINVENT ⁵³	0.480 ± 0.344	0.213 ± 0.081	2.453 ± 0.561	0.127 ± 0.088	0.613 ± 0.167
MORLD ⁵⁴	0.047 ± 0.050	0.007 ± 0.013	0.880 ± 0.735	0.047 ± 0.040	0.227 ± 0.118
HierVAE ⁵⁵	0.553 ± 0.214	0.007 ± 0.013	0.507 ± 0.278	0.207 ± 0.220	0.227 ± 0.127
FREED ⁵⁶	3.627 ± 0.961	1.107 ± 0.209	10.187 ± 3.306	2.067 ± 0.626	4.520 ± 0.673
GDSS ⁵⁷	1.933 ± 0.208	0.368 ± 0.103	4.667 ± 0.306	0.167 ± 0.134	1.167 ± 0.281
MOOD ⁹	$\underline{7.017 \pm 0.428}$	0.733 ± 0.141	$\mathbf{18.673 \pm 0.423}$	$\underline{5.240 \pm 0.285}$	$\underline{9.200 \pm 0.524}$
ChemBFN strategy 3	4.893 ± 0.596	$\underline{5.426 \pm 0.542}$	5.960 ± 0.505	4.740 ± 0.329	5.367 ± 0.426
ChemBFN strategy 4	$\mathbf{8.980 \pm 0.186}$	$\mathbf{5.993 \pm 0.191}$	11.940 ± 0.638	$\mathbf{12.573 \pm 0.569}$	$\mathbf{9.827 \pm 0.570}$

^a The best results are in **bold** and the second best results are underlined. \uparrow stands for the higher the better. We sampled the molecules with ODE-like generating process for 100 steps in **SMILES** format. The results were the average values of 5 runs with the standard deviation reported.

Table 6: Novel top 5% docking scores (\downarrow) of ChemBFN + RL + ODE-like sampling ($\tau = 0.5$) compared with SOTA models^a

Methods	PARP1	FA7	Target proteins		
			5HT1B	BRAF	JAK2
REINVENT ⁵³	-8.702 ± 0.523	-7.205 ± 0.264	-8.770 ± 0.316	-8.392 ± 0.400	-8.165 ± 0.277
MORLD ⁵⁴	-7.532 ± 0.260	-6.263 ± 0.165	-7.869 ± 0.650	-8.040 ± 0.337	-7.816 ± 0.133
HierVAE ⁵⁵	-9.487 ± 0.278	-6.812 ± 0.274	-8.081 ± 0.252	-8.978 ± 0.525	-8.285 ± 0.370
FREED ⁵⁶	-10.427 ± 0.177	-8.297 ± 0.094	-10.425 ± 0.331	-10.325 ± 0.164	-9.624 ± 0.102
GDSS ⁵⁷	-9.967 ± 0.028	-7.775 ± 0.039	-9.459 ± 0.101	-9.224 ± 0.068	-8.926 ± 0.089
MOOD ⁹	-10.865 ± 0.113	-8.160 ± 0.071	-11.145 ± 0.042	-11.063 ± 0.034	-10.147 ± 0.060
ChemBFN strategy 3	$\mathbf{-12.533 \pm 0.200}$	$\mathbf{-9.383 \pm 0.093}$	$\mathbf{-12.518 \pm 0.162}$	$\mathbf{-12.019 \pm 0.170}$	$\mathbf{-11.861 \pm 0.190}$
ChemBFN strategy 4	$\underline{-12.092 \pm 0.120}$	$\underline{-8.929 \pm 0.097}$	$\underline{-11.949 \pm 0.093}$	$\underline{-11.715 \pm 0.075}$	$\underline{-12.181 \pm 0.198}$

^a \downarrow stands for the lower the better while other settings are the same as Table 5

Table 7: Novel hit ratios (\uparrow) compared with SOTA models^a

Methods	PARP1	FA7	Target proteins		JAK2
			5HT1B	BRAF	
REINVENT ⁵³	0.480 ± 0.344	0.213 ± 0.081	2.453 ± 0.561	0.127 ± 0.088	0.613 ± 0.167
MORLD ⁵⁴	0.047 ± 0.050	0.007 ± 0.013	0.880 ± 0.735	0.047 ± 0.040	0.227 ± 0.118
HierVAE ⁵⁵	0.553 ± 0.214	0.007 ± 0.013	0.507 ± 0.278	0.207 ± 0.220	0.227 ± 0.127
FREED ⁵⁶	3.627 ± 0.961	1.107 ± 0.209	10.187 ± 3.306	2.067 ± 0.626	4.520 ± 0.673
GDSS ⁵⁷	1.933 ± 0.208	0.368 ± 0.103	4.667 ± 0.306	0.167 ± 0.134	1.167 ± 0.281
MOOD ⁹	7.017 ± 0.428	0.733 ± 0.141	18.673 ± 0.423	5.240 ± 0.285	9.200 ± 0.524
ChemBFN strategy 3	$\underline{31.547} \pm 0.730$	$\mathbf{31.460} \pm 0.858$	25.047 ± 0.837	26.893 ± 1.022	34.060 ± 0.710
ChemBFN strategy 4	$\mathbf{33.240} \pm 1.018$	30.133 ± 0.442	$\mathbf{30.933} \pm 0.573$	29.033 ± 0.647	42.133 ± 1.509

^a The best results are in **bold** and the second best results are underlined. \uparrow stands for the higher the better. We sampled the molecules for 1,000 steps in **SELFIES** format. The results were the average values of 5 runs with the standard deviation reported.

 Table 8: Novel top 5% docking scores (\downarrow) compared with SOTA models^a

Methods	PARP1	FA7	Target proteins		JAK2
			5HT1B	BRAF	
REINVENT ⁵³	-8.702 ± 0.523	-7.205 ± 0.264	-8.770 ± 0.316	-8.392 ± 0.400	-8.165 ± 0.277
MORLD ⁵⁴	-7.532 ± 0.260	-6.263 ± 0.165	-7.869 ± 0.650	-8.040 ± 0.337	-7.816 ± 0.133
HierVAE ⁵⁵	-9.487 ± 0.278	-6.812 ± 0.274	-8.081 ± 0.252	-8.978 ± 0.525	-8.285 ± 0.370
FREED ⁵⁶	-10.427 ± 0.177	-8.297 ± 0.094	-10.425 ± 0.331	-10.325 ± 0.164	-9.624 ± 0.102
GDSS ⁵⁷	-9.967 ± 0.028	-7.775 ± 0.039	-9.459 ± 0.101	-9.224 ± 0.068	-8.926 ± 0.089
MOOD ⁹	-10.865 ± 0.113	-8.160 ± 0.071	-11.145 ± 0.042	-11.063 ± 0.034	-10.147 ± 0.060
ChemBFN strategy 3	$\mathbf{-12.455} \pm 0.068$	$\mathbf{-9.527} \pm 0.033$	$\mathbf{-12.609} \pm 0.045$	-12.043 ± 0.117	$\mathbf{-11.690} \pm 0.105$
ChemBFN strategy 4	$\underline{-12.358} \pm 0.102$	$\underline{-9.315} \pm 0.026$	$\underline{-12.359} \pm 0.172$	$\mathbf{-12.061} \pm 0.087$	-11.666 ± 0.089

^a \downarrow stands for the lower the better while other settings are the same as Table 7

Examples of novel hit molecules generated by our model (both SMILES version and SELFIES version) were illustrated in Figure 6 and Figure 7. An interesting observation is that although the ring systems in the training data are generally small, our model tended to generate larger ring systems or even macrocyclic systems that showed lower binding energies.

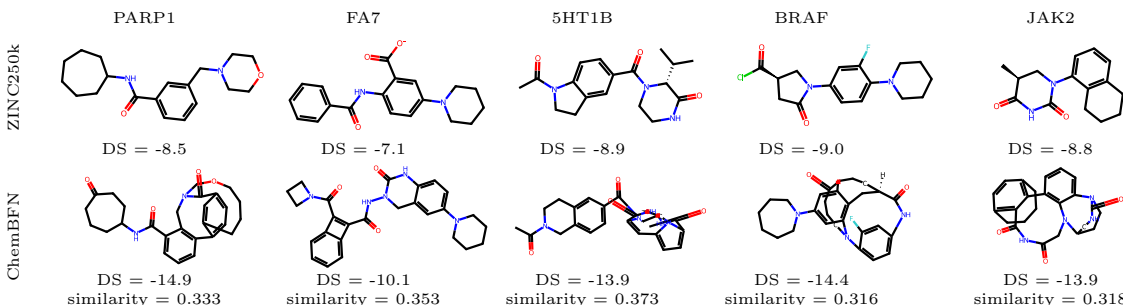


Figure 6: Examples of novel hit molecules generated by ChemBFN (SMILES version) against their closest neighbours in the training space.

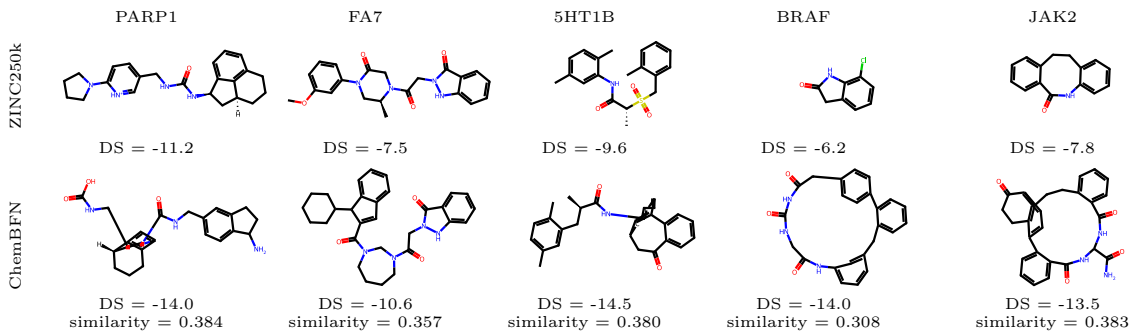


Figure 7: Examples of novel hit molecules generated by ChemBFN (SELFIES version) against their closest neighbours in the training space.

Conditional Generation of Protein Sequences

An amino acid-wise tokenizer was added to the original ChemBFN model to enable protein sequence generating. We trained one model to optimise the percentage of beta sheets and one model to optimise SASA. Each model, after training, generated 32×2 protein sequences (half was generated via strategy 3 and half via strategy 4) guided by an objective value pointing to the high property regions. As shown in Figure 8, the generated samples all had higher objective values than the training space. When estimated the naturalness (ProtGPT2⁵⁸ log likelihood as suggested by N. Gruver *et al*⁵⁰) of the generated proteins, we found that models utilising either strategy 3 or strategy 4 gave reasonably acceptable results compared with natural proteins (see Figure 8). As SASA and the percentage of beta sheets of proteins are highly correlated their structures, we conclude that our model is capable of determining the relationship between an objective (scalar) value to its corresponding chemical structures, unsupervised, and extrapolating to unseen spaces.

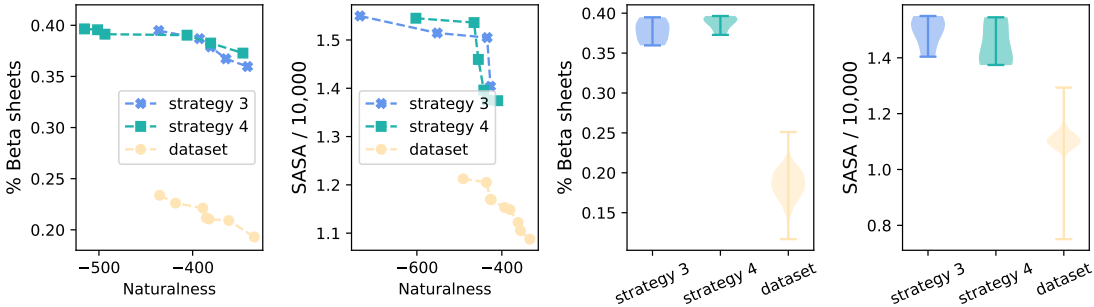


Figure 8: (Left 2 plots) The Pareto fronts of objective values *v.s.* naturalness of generated protein sequences and dataset; (Right 2 plots) The violin plots of the objective values of generated samples and dataset. Notice that our method generated proteins with higher objective values than any entity in the training dataset while maintaining the similar naturalness to natural proteins.

What If You Care More About In-Distribution Sampling

In this section, we demonstrate how pre-training affects the sampling distributions of MOSES as an example. Finetuned models based on models, provided by N. Tao *et al.*³⁵ pretrained on 40M and 190M molecules selected from ZINC15 database⁵⁹ were denoted as ‘finetuned 1’ and ‘finetuned 2’, respectively. As shown in Figure 9, the increasing of pre-training data surprisingly led to the decrease of FCD metrics. However, when applying LoRA⁶⁰ finetune strategy (rank = 4, α = 1) to the pretrainind model (pretrained on 190M molecules), both FCD and the ratio of novel generated molecules increased while the ratio of molecules which passed the MOSES benchmark filters decreased. We conclude here that larger scale pre-training helps to obtain generated molecules closer to the training space only when all the parameters of the network were finetuned; on the other hand, LoRA finetuning, i.e., reduced parameter finetuning, will further strengthen the OOD-ness.

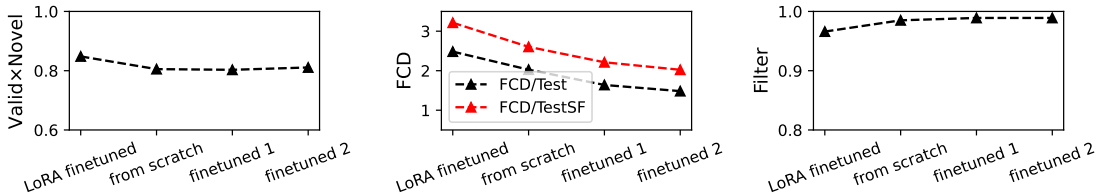


Figure 9: The key MOSES testing metrics of finetuned models. We reported Valid \times Novel values instead of validity and novelty separately. Note that we employed strategy 1 in this experiment.

Computational Details

All the models were trained on single Nvidia A100 GPU with a batch-size of 120 for MOSES and GuacaMol datasets and 128 for ZINC250k and protein datasets for 100 epochs. The learning rate was 5×10^{-5} which was linearly increased from 10^{-8} during the first 1,000 steps. AdamW⁶¹ method with default parameters was employed to optimise the model weights. A unconditional rate of 0.2 was chosen when training conditional models. During sampling process, the batch-size was 3,000 for small molecules and 32 for protein sequences; the guidance strength was 0.5 for small molecules and 1.0 for protein sequences when a guidance vector was applied. The number of sampling steps, if not being specified, was 100 for MOSES while 1,000 for GuacaMol, ZINC250k and protein sequences. The models trained for generating small molecules had 12 layers, 8 attention heads per layer and 512 hidden feature sizes (54.5M of total parameters); the models for protein sequences had 12 layers, 16 attention heads per layer and 1,024 hidden feature sizes (216M of total parameters).

RDKit⁶² was used to generate 3-dimensional conformations and Margon fingerprint (radius = 2, dimension = 1024) from SMILES strings and calculate the Tanimoto similarity, QED, and SA quantities. The docking scores were computed via QuickVina 2.⁴⁹ The properties of proteins were calculate via Biopython⁶³ package version 1.84; to obtain the solvent accessible surface area, the 3-dimensional structures were predicted by ESMFold⁶⁴ model first, which was followed by Shrake-and-Rupley algorithm⁶⁵ calculations.

In order to generate UMAP plots, the vector molecular representations were extracted from the last activation layer of ChemNet,⁴⁵ which were later projected to 2-dimensional vectors by UMAP package.⁵¹ 5,000 random molecules were selected from the dataset as the representatives.

Conclusion

In this research, we showed that BFN, especially ChemBFN model, is naturally a controllable out-of-distribution sampler, which is versatile to generate both small molecules and large chemical systems such as proteins. We found that for unconditional generation, the normal training-SAR sampling strategy promoted the OOD-ness of the model most; when a guidance was switched on, the OOD behaviour was pushed to a higher level, in which case the SAR trained models outperformed several state-of-the-art methods: the SAR training-normal sampling strategy tended to samples with higher objective values while the SAR training-SAR sampling strategy had a tendency to yield more novel samples. The generated samples in the OOD regions satisfied several real-world requirements including high drug-likeness, low synthetic difficulties, and similar naturalness to their natural counterparts, which makes our method a strong candidate to handle *de novo* drug design challenges. In addition, we developed strategies to reduce the inferencing time which makes ChemBFN more cost efficient in large scale sampling.

Data and Software Availability

The code of ChemBFN and instructions necessary to reproduce the results of this study are available for downloading at:

<https://github.com/Augus1999/bayesian-flow-network-for-chemistry>.

Acknowledgements

The computational source of GPU was provided by Research Center for Computational Science, Okazaki, Japan (Project: 24-IMS-C043).

Conflict of Interest

The author claim no conflicts of interest.

Funding Sources

The authors claim that there is no funding related to this research.

References

- (1) Bohacek, R. S.; McMartin, C.; Guida, W. C. The art and practice of structure-based drug design: a molecular modeling perspective. *Medicinal research reviews* **1996**, *16*, 3–50.
- (2) Ertl, P. Cheminformatics analysis of organic substituents: identification of the most common substituents, calculation of substituent properties, and automatic identification of drug-like bioisosteric groups. *Journal of chemical information and computer sciences* **2003**, *43*, 374–380.
- (3) Reymond, J.-L.; van Deursen, R.; Blum, L. C.; Ruddigkeit, L. Chemical space as a source for new drugs. *Med. Chem. Commun.* **2010**, *1*, 30–38.
- (4) Abdelraheem, E. M.; Shaabani, S.; Dömling, A. Macrocycles: MCR synthesis and applications in drug discovery. *Drug Discovery Today: Technologies* **2018**, *29*, 11–17.
- (5) Garcia Jimenez, D.; Poongavanam, V.; Kihlberg, J. Macrocycles in Drug Discovery—Learning from the Past for the Future. *Journal of Medicinal Chemistry* **2023**, *66*, 5377–5396, PMID: 37017513.
- (6) Driggers, E. M.; Hale, S. P.; Lee, J.; Terrett, N. K. The exploration of macrocycles

for drug discovery—an underexploited structural class. *Nature Reviews Drug Discovery* **2008**, *7*, 608–624.

(7) Maynard Smith, J. Natural selection and the concept of a protein space. *Nature* **1970**, *225*, 563–564.

(8) Gómez-Bombarelli, R.; Wei, J. N.; Duvenaud, D.; Hernández-Lobato, J. M.; Sánchez-Lengeling, B.; Sheberla, D.; Aguilera-Iparraguirre, J.; Hirzel, T. D.; Adams, R. P.; Aspuru-Guzik, A. Automatic chemical design using a data-driven continuous representation of molecules. *ACS central science* **2018**, *4*, 268–276.

(9) Lee, S.; Jo, J.; Hwang, S. J. Exploring Chemical Space with Score-based Out-of-distribution Generation. 2023; <https://arxiv.org/abs/2206.07632>.

(10) Lim, J.; Ryu, S.; Kim, J. W.; Kim, W. Y. Molecular generative model based on conditional variational autoencoder for de novo molecular design. *Journal of cheminformatics* **2018**, *10*, 31.

(11) Schwalbe-Koda, D.; Gómez-Bombarelli, R. *Machine Learning Meets Quantum Physics*; Springer International Publishing, 2020; p 445–467.

(12) Zhung, W.; Kim, H.; Kim, W. Y. 3D molecular generative framework for interaction-guided drug design. *Nature Communications* **2024**, *15*, 2688.

(13) Walters, W. P.; Murcko, M. Assessing the impact of generative AI on medicinal chemistry. *Nature biotechnology* **2020**, *38*, 143–145.

(14) Klarner, L.; Rudner, T. G. J.; Morris, G. M.; Deane, C. M.; Teh, Y. W. Context-Guided Diffusion for Out-of-Distribution Molecular and Protein Design. 2024; <https://arxiv.org/abs/2407.11942>.

(15) Ho, J.; Jain, A.; Abbeel, P. Denoising diffusion probabilistic models. *Advances in neural information processing systems* **2020**, *33*, 6840–6851.

(16) Song, J.; Meng, C.; Ermon, S. Denoising Diffusion Implicit Models. 2022; <https://arxiv.org/abs/2010.02502>.

(17) Sohl-Dickstein, J.; Weiss, E.; Maheswaranathan, N.; Ganguli, S. Deep Unsupervised Learning using Nonequilibrium Thermodynamics. Proceedings of the 32nd International Conference on Machine Learning. Lille, France, 2015; pp 2256–2265.

(18) Song, Y.; Sohl-Dickstein, J.; Kingma, D. P.; Kumar, A.; Ermon, S.; Poole, B. Score-Based Generative Modeling through Stochastic Differential Equations. 2021; <https://arxiv.org/abs/2011.13456>.

(19) Bortoli, V. D.; Thornton, J.; Heng, J.; Doucet, A. Diffusion Schrödinger Bridge with Applications to Score-Based Generative Modeling. 2023; <https://arxiv.org/abs/2106.01357>.

(20) Frans, K.; Hafner, D.; Levine, S.; Abbeel, P. One Step Diffusion via Shortcut Models. 2024; <https://arxiv.org/abs/2410.12557>.

(21) Lipman, Y.; Chen, R. T. Q.; Ben-Hamu, H.; Nickel, M.; Le, M. Flow Matching for Generative Modeling. 2023; <https://arxiv.org/abs/2210.02747>.

(22) Albergo, M. S.; Boffi, N. M.; Vanden-Eijnden, E. Stochastic Interpolants: A Unifying Framework for Flows and Diffusions. 2023; <https://arxiv.org/abs/2303.08797>.

(23) Tong, A.; Fatras, K.; Malkin, N.; Huguet, G.; Zhang, Y.; Rector-Brooks, J.; Wolf, G.; Bengio, Y. Improving and generalizing flow-based generative models with minibatch optimal transport. 2024; <https://arxiv.org/abs/2302.00482>.

(24) Dunn, I.; Koes, D. R. Mixed Continuous and Categorical Flow Matching for 3D De Novo Molecule Generation. 2024; <https://arxiv.org/abs/2404.19739>.

(25) Stark, H.; Jing, B.; Wang, C.; Corso, G.; Berger, B.; Barzilay, R.; Jaakkola, T. Dirichlet

Flow Matching with Applications to DNA Sequence Design. 2024; <https://arxiv.org/abs/2402.05841>.

(26) Davis, O.; Kessler, S.; Petracche, M.; İsmail İlkan Ceylan; Bronstein, M.; Bose, A. J. Fisher Flow Matching for Generative Modeling over Discrete Data. 2024; <https://arxiv.org/abs/2405.14664>.

(27) Cheng, C.; Li, J.; Peng, J.; Liu, G. Categorical Flow Matching on Statistical Manifolds. 2025; <https://arxiv.org/abs/2405.16441>.

(28) Gat, I.; Remez, T.; Shaul, N.; Kreuk, F.; Chen, R. T. Q.; Synnaeve, G.; Adi, Y.; Lipman, Y. Discrete Flow Matching. 2024; <https://arxiv.org/abs/2407.15595>.

(29) Dunn, I.; Koes, D. R. Exploring Discrete Flow Matching for 3D De Novo Molecule Generation. 2024; <https://arxiv.org/abs/2411.16644>.

(30) Graves, A.; Srivastava, R. K.; Atkinson, T.; Gomez, F. Bayesian Flow Networks. 2024; <https://arxiv.org/abs/2308.07037>.

(31) Xue, K.; Zhou, Y.; Nie, S.; Min, X.; Zhang, X.; Zhou, J.; Li, C. Unifying Bayesian Flow Networks and Diffusion Models through Stochastic Differential Equations. 2024; <https://arxiv.org/abs/2404.15766>.

(32) Atkinson, T.; Barrett, T. D.; Cameron, S.; Guloglu, B.; Greenig, M.; Robinson, L.; Graves, A.; Copoiu, L.; Laterre, A. Protein Sequence Modelling with Bayesian Flow Networks. 2024; <https://www.biorxiv.org/content/early/2024/09/26/2024.09.24.614734>.

(33) Song, Y.; Gong, J.; Zhou, H.; Zheng, M.; Liu, J.; Ma, W.-Y. Unified Generative Modeling of 3D Molecules with Bayesian Flow Networks. The Twelfth International Conference on Learning Representations. 2024.

(34) Qu, Y.; Qiu, K.; Song, Y.; Gong, J.; Han, J.; Zheng, M.; Zhou, H.; Ma, W.-Y. MolCRAFT: Structure-Based Drug Design in Continuous Parameter Space. 2024; <https://arxiv.org/abs/2404.12141>.

(35) Tao, N.; Abe, M. Bayesian Flow Network Framework for Chemistry Tasks. *Journal of Chemical Information and Modeling* **2025**, PMID: 39836530.

(36) Weininger, D. SMILES, a chemical language and information system. 1. Introduction to methodology and encoding rules. *Journal of chemical information and computer sciences* **1988**, *28*, 31–36.

(37) Krenn, M.; Häse, F.; Nigam, A.; Friederich, P.; Aspuru-Guzik, A. Self-referencing embedded strings (SELFIES): A 100% robust molecular string representation. *Machine Learning: Science and Technology* **2020**, *1*, 045024.

(38) Williams, R. J. Simple statistical gradient-following algorithms for connectionist reinforcement learning. *Machine learning* **1992**, *8*, 229–256.

(39) Sutton, R. S.; McAllester, D.; Singh, S.; Mansour, Y. Policy gradient methods for reinforcement learning with function approximation. *Advances in neural information processing systems* **1999**, *12*, 1057–1063.

(40) Devlin, J.; Chang, M.-W.; Lee, K.; Toutanova, K. BERT: Pre-training of Deep Bidirectional Transformers for Language Understanding. 2019; <https://arxiv.org/abs/1810.04805>.

(41) Vaswani, A.; Shazeer, N.; Parmar, N.; Uszkoreit, J.; Jones, L.; Gomez, A. N.; Kaiser, L.; Polosukhin, I. Attention Is All You Need. 2023; <https://arxiv.org/abs/1706.03762>.

(42) Yenduri, G.; M, R.; G, C. S.; Y, S.; Srivastava, G.; Maddikunta, P. K. R.; G, D. R.; Jhaveri, R. H.; B, P.; Wang, W.; Vasilakos, A. V.; Gadekallu, T. R. Generative Pre-trained Transformer: A Comprehensive Review on Enabling Technologies, Potential

Applications, Emerging Challenges, and Future Directions. 2023; <https://arxiv.org/abs/2305.10435>.

- (43) Polykovskiy, D. et al. Molecular Sets (MOSES): A Benchmarking Platform for Molecular Generation Models. 2020; <https://arxiv.org/abs/1811.12823>.
- (44) Brown, N.; Fiscato, M.; Segler, M. H.; Vaucher, A. C. GuacaMol: benchmarking models for de novo molecular design. *Journal of chemical information and modeling* **2019**, *59*, 1096–1108.
- (45) Preuer, K.; Renz, P.; Unterthiner, T.; Hochreiter, S.; Klambauer, G. Fréchet ChemNet Distance: A Metric for Generative Models for Molecules in Drug Discovery. *Journal of Chemical Information and Modeling* **2018**, *58*, 1736–1741, PMID: 30118593.
- (46) Irwin, J. J.; Shoichet, B. K. ZINC- a free database of commercially available compounds for virtual screening. *Journal of chemical information and modeling* **2005**, *45*, 177–182.
- (47) Bickerton, G. R.; Paolini, G. V.; Besnard, J.; Muresan, S.; Hopkins, A. L. Quantifying the chemical beauty of drugs. *Nature chemistry* **2012**, *4*, 90–98.
- (48) Ertl, P.; Schuffenhauer, A. Estimation of synthetic accessibility score of drug-like molecules based on molecular complexity and fragment contributions. *Journal of cheminformatics* **2009**, *1*, 8.
- (49) Alhossary, A.; Handoko, S. D.; Mu, Y.; Kwoh, C.-K. Fast, accurate, and reliable molecular docking with QuickVina 2. *Bioinformatics* **2015**, *31*, 2214–2216.
- (50) Gruver, N.; Stanton, S.; Frey, N.; Rudner, T. G. J.; Hotzel, I.; Lafrance-Vanassee, J.; Rajpal, A.; Cho, K.; Wilson, A. G. Protein design with guided discrete diffusion. Proceedings of the 37th International Conference on Neural Information Processing Systems. Red Hook, NY, USA, 2024.

(51) McInnes, L.; Healy, J.; Melville, J. UMAP: Uniform Manifold Approximation and Projection for Dimension Reduction. 2020; <https://arxiv.org/abs/1802.03426>.

(52) Ho, J.; Salimans, T. Classifier-Free Diffusion Guidance. 2022; <https://arxiv.org/abs/2207.12598>.

(53) Olivecrona, M.; Blaschke, T.; Engkvist, O.; Chen, H. Molecular de-novo design through deep reinforcement learning. *Journal of cheminformatics* **2017**, *9*, 48.

(54) Jeon, W.; Kim, D. Autonomous molecule generation using reinforcement learning and docking to develop potential novel inhibitors. *Scientific reports* **2020**, *10*, 22104.

(55) Jin, W.; Barzilay, D.; Jaakkola, T. Hierarchical Generation of Molecular Graphs using Structural Motifs. Proceedings of the 37th International Conference on Machine Learning. 2020; pp 4839–4848.

(56) Yang, S.; Hwang, D.; Lee, S.; Ryu, S.; Hwang, S. J. Hit and Lead Discovery with Explorative RL and Fragment-based Molecule Generation. 2021; <https://arxiv.org/abs/2110.01219>.

(57) Jo, J.; Lee, S.; Hwang, S. J. Score-based Generative Modeling of Graphs via the System of Stochastic Differential Equations. 2022; <https://arxiv.org/abs/2202.02514>.

(58) Ferruz, N.; Schmidt, S.; Höcker, B. ProtGPT2 is a deep unsupervised language model for protein design. *Nature communications* **2022**, *13*, 4348.

(59) Sterling, T.; Irwin, J. J. ZINC 15–ligand discovery for everyone. *Journal of chemical information and modeling* **2015**, *55*, 2324–2337.

(60) Hu, E. J.; Shen, Y.; Wallis, P.; Allen-Zhu, Z.; Li, Y.; Wang, S.; Wang, L.; Chen, W. LoRA: Low-Rank Adaptation of Large Language Models. International Conference on Learning Representations. 2022.

(61) Loshchilov, I.; Hutter, F. Fixing Weight Decay Regularization in Adam. 2019; <https://arxiv.org/abs/1711.05101>.

(62) RDKit: Open-source cheminformatics. <https://www.rdkit.org>, Accessed: 2024-11-12.

(63) Cock, P. J. A.; Antao, T.; Chang, J. T.; Chapman, B. A.; Cox, C. J.; Dalke, A.; Friedberg, I.; Hamelryck, T.; Kauff, F.; Wilczynski, B.; de Hoon, M. J. L. Biopython: freely available Python tools for computational molecular biology and bioinformatics. *Bioinformatics* **2009**, *25*, 1422–1423.

(64) Lin, Z.; Akin, H.; Rao, R.; Hie, B.; Zhu, Z.; Lu, W.; Smetanin, N.; dos Santos Costa, A.; Fazel-Zarandi, M.; Sercu, T.; Candido, S.; others Language models of protein sequences at the scale of evolution enable accurate structure prediction. 2022.

(65) Shrake, A.; Rupley, J. A. Environment and exposure to solvent of protein atoms. Lysozyme and insulin. *Journal of molecular biology* **1973**, *79*, 351–371.

TOC Graphic

